

# The study of chiral discrimination of organophosphonate derivatives on pirkle type chiral stationary phase by molecular modeling

Guo-Sheng Yang<sup>a,b</sup>, Shi-Ling Yuan<sup>b</sup>, Xian-Jie Lin<sup>b</sup>, Zhong-Nan Qi<sup>b</sup>,  
Cheng-Bu Liu<sup>b</sup>, Hassan Y. Aboul-Enein<sup>c,\*</sup>, Guy Félix<sup>d</sup>

<sup>a</sup> Shandong Key Laboratory of Chemical Function Materials, Shandong Normal University, Jinan 250014, PR China

<sup>b</sup> Department of Chemistry, Shandong University, Jinan 250100, PR China

<sup>c</sup> Pharmaceutical Analysis Laboratory, Biological and Medical Research Department (MBC 03-65),  
King Faisal Specialist Hospital and Research Centre, P.O. Box 3354, Riyadh 11211, Saudi Arabia

<sup>d</sup> Laboratoire de Chimie Organique et Matériaux Moléculaires (UMR 6114), Faculté des Sciences de Luminy,  
163 Avenue de Luminy, 13 288 Marseille Cedex 9, France

Received 30 October 2003; received in revised form 9 February 2004; accepted 17 February 2004

Available online 11 May 2004

## Abstract

Molecular modeling and molecular dynamics (MD) have been used to study the chiral discrimination and interaction energy of organophosphonate in *N*-(3,5-dinitrobenzoyl)-*S*-leucine chiral stationary phase (CSP). The elution order of the enantiomers can be predicted from the interaction energy. Quantitative structure-retention relationship (QSRR) has also been used as an alternative method to confirm the elution order of enantiomers. Molecular mechanics (MM), molecular dynamics and QSRR proved to be useful methods to study chiral discrimination. © 2004 Elsevier B.V. All rights reserved.

**Keywords:** Chiral discrimination; Molecular modeling; Molecular dynamics; QSRR; Organophosphonate derivatives; *N*-(3,5-dinitrobenzoyl)-*L*-leucine chiral stationary phase

## 1. Introduction

Chirality has been thrust to the scientific forefront in several sub-disciplines of the chemical sciences, particularly in organic, biological and pharmaceutical chemistry [1,2]. Separations scientists have understood for many years that by using a suitable chiral environment, either a stationary phase or a mobile phase additive, one should be able to carry out a direct separation on the chromatographic column without the need of generating diastereomers as intermediates. Enormous advances have been made in such separations in the past decade and nowadays a wide range of chromatographic columns and additives are available for use in planar chromatography, gas-, liquid-, super and subcritical fluid chromatographies and capillary electrophoresis [3,4]. In spite of these advances a redundant question often heard special concerning these chromatographic systems is: “how

do they work?” To address this question a significant number of experimentalists as well as molecular modelers have carried out computational studies on the competing transient diastereomeric complexes involved in enantiodifferentiation to understand how the inter-molecular forces work, in concert, to give rise to chiral separations [5,6].

In Pirkle's type chiral phases, the chiral discrimination was based on three interactions between enantiomers and chiral phases. A typical case is when a bulky group is bonded to the chiral center, the interaction is possible if one of the enantiomers forms a perfect steric fit and affords favorable van der Waal's interactions with this bulky group. Accordingly, the stereoselectivity obtained is due to two attractive interactions of  $\pi$ – $\pi$  interaction and H-bonding, together with a steric interaction [7]. Still and Rogers [8] assessed the distribution of conformers for the analyte and the chiral stationary phase (CSP) analogs using the MM2 force field. Several docking strategies were employed but only the most stable structures from their conformational analysis were used to form the initial binary complexes. The docking strategies were based on previously determined NMR chemical

\* Corresponding author. Tel.: +966-1-442-78-59;

fax: +966-1-442-78-58.

E-mail address: [enein@kfshrc.edu.sa](mailto:enein@kfshrc.edu.sa) (H.Y. Aboul-Enein).

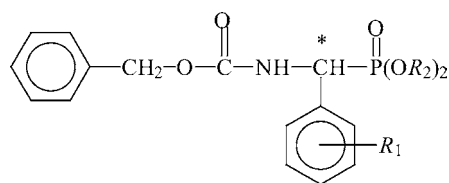


Fig. 1. The general structure of *O,O*-dialkyl-1-benzyloxycarbonyl-aminoaryl methyl phosphonate used in this study. Asterisk (\*) denotes the position of chiral carbon.

shifts. Using MM2 in all examples Lipkowitz and coworkers [9–12] were able to predict the correct retention order (i.e., the sign of  $\Delta G$  was always correct) and when their differential free energies were converted to separation factors,  $\alpha$ , plots of computed versus observed  $\alpha$  were linear and usually with high correlation coefficients. We also studied the chiral discrimination of diniconazole in Sumichiral OA4700 column which is a Pirkle type chiral stationary phase made of *S*-tert-leucine covalently bound to *S*-1-( $\alpha$ -naphthyl) ethyl amine. Using MM2, we got the most stable structures of chiral stationary phase and diniconazole enantiomers and optimized the conformations of complexes (*R*-CSP and *S*-CSP). The elution order of enantiomers was determined from the energy of the *R*-CSP and *S*-CSP complexes [13].

In this paper, we report the study of chiral discrimination of organophosphonate derivatives (Fig. 1) on *N*-(3,5-dinitrobenzoyl)-*S*-leucine chiral stationary phase by molecular modeling. Using molecular modeling, molecular dynamics (MD), we can predict the chiral discrimination position, the energy of the complex of CSP and enantiomers. From the energy, we can determine the elution order of the enantiomer. Furthermore, quantitative structure-retention relationship (QSRR) is applied as an alternative method to confirm the elution order of enantiomers. The computational results were obtained by the Silicon Graphics Indigo workstation Origin 300 with the software of molecular mechanics (MM), molecular dynamics and QSAR in programs Cerius<sup>2</sup> from MSI (Molecular Simulations Inc., San Diego).

## 2. Experimental

### 2.1. Materials

A series of fifteen dialkyl-benzyloxycarbonyl-aminoaryl-methyl phosphonate compounds were synthesized by the National Laboratory of Elemento-Organic Chemistry, Nankai University [14]. The general structure of the compounds is presented in Fig. 1. The structures of the substituents “*R*<sub>1</sub>” are H, CH<sub>3</sub>, NO<sub>2</sub>, OCH<sub>3</sub> and Cl, respectively. The substituents “*R*<sub>2</sub>” are Me, Et, Pr and *i*-Pr. These compounds were dissolved in ethanol and then diluted with the eluent solvent. Solutions with approximate concentration of 1 mg mL<sup>-1</sup> in eluent solvent were used for injection. All solvents were filtered by a 0.5  $\mu$ m filter and degassed in vacuum before use.

### 2.2. Apparatus

The chromatography was performed with Shimadzu (Japan) modular liquid chromatography equipped with HP3394A integrator, SPD-10A UV-Vis detector and LC-10AD solvent delivery system.

### 2.3. Chromatography conditions

*N*-(3,5-dinitrobenzoyl)-*L*-leucine chiral stationary phase was synthesized according to Gao et al. [15] and packed into a 250 mm  $\times$  4.6 mm i.d. stainless steel column. The mobile phase was different compositions of isopropanol in *n*-hexane. The flow-rate was maintained at 1 mL min<sup>-1</sup>. SPD-10A UV-Vis detector was at 230 nm.

### 2.4. Theory and methods

#### 2.4.1. Molecular modeling

In chiral separation, there are interactions between chiral stationary phase and analyte to form the transient diastereomeric complexes as follows:



where CSP is the chiral stationary phase, A-*R* and A-*S* the *R* and *S* enantiomers of analyte A, CSP·A-*R* and CSP·A-*S* are the complex of chiral stationary phase and the *R*- and *S*-enantiomers of analyte, respectively. The retention time (*T*<sub>r</sub>) of analyte *R* and *S* depends on the energy of the complex. If there is a more stable complex, it will possess a longer retention time.

$$\ln T_r \alpha - \Delta G_{\text{CSP} \cdot \text{A}} \quad (3)$$

$$-\Delta G_{\text{CSP} \cdot \text{A}} = E_{\text{CSP} \cdot \text{A}} - (E_{\text{CSP}} + E_{\text{A}}) \quad (4)$$

$$-\Delta G_{\text{CSP} \cdot \text{A}-R} = E_{\text{CSP} \cdot \text{A}-R} - (E_{\text{CSP}} + E_{\text{A}-R}) \quad (5)$$

$$-\Delta G_{\text{CSP} \cdot \text{A}-S} = E_{\text{CSP} \cdot \text{A}-S} - (E_{\text{CSP}} + E_{\text{A}-S}) \quad (6)$$

In this study, we calculate the energy of chiral stationary phase as a molecule (Fig. 2A) instead of the energy of the bonded silica chiral stationary phase (Fig. 2B). The energy of complex CSP·A-*R* and CSP·A-*S* are calculated based on the auto-docking function of the program.

The calculation of energy was based on universal force field (UFF) in programs Cerius<sup>2</sup> [16,17]. The total energy (*E*<sub>T</sub>) composed by the energy of bonds (*E*<sub>bond</sub>), angles (*E*<sub>ang</sub>), torsions (*E*<sub>tor</sub>), electrostatic (*E*<sub>ele</sub>), inversions (*E*<sub>inv</sub>) and van der Waal (*E*<sub>VDW</sub>)

$$E_T = E_{\text{bond}} + E_{\text{ang}} + E_{\text{tor}} + E_{\text{ele}} + E_{\text{inv}} + E_{\text{VDW}} \quad (7)$$

After building the structures, we can use the function to minimize the energy under UFF. The maximum number of interactions is 5000. For the interaction of organophosphonate derivatives and chiral stationary phase, we calculate the

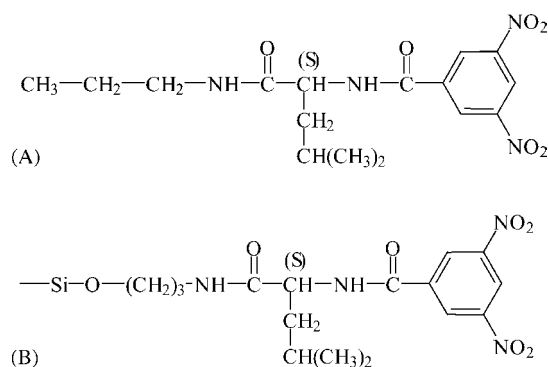


Fig. 2. The structure of (A) *N*-(3,5-dinitrobenzoyl)-leucine and (B) *N*-(3,5-dinitrobenzoyl)-leucine chiral stationary phase.

two minimized structures individually at first, then, minimize the energy of the two molecules to get the energy of the complex. After 5000 steps at 0.0010 ps for each step of dynamics simulation at 300 K, we minimize the energy again. This represents the final energy of the complex of organophosphonate derivatives and chiral stationary phase.

From the energy of  $-\Delta G_{\text{CSP.A-R}}$  and  $-\Delta G_{\text{CSP.A-S}}$ , one can determine which of the enantiomers has longer retention time.

#### 2.4.2. The quantitative structure-retention relationship (QSRR)

For the elution order of the enantiomers of this series of organophosphonate derivatives, we applied QSRR as an alternative method to confirm our results. Quantitative structure-retention relationship is a multi-variant statistical correlation between the retention time and the key geometrical or chemical characteristics of a molecular system.

The computational results were obtained using a Silicon Graphics Indigo workstation, and the software programs Cerius2 and QSAR from MSI (Molecular Simulations Inc.,

San Diego, CA, USA). In the program package, the micro-structures like area, dipole and lowest unoccupied molecular orbital energy (LUMO) were calculated. We used the Visualizer model to build the molecular structure, then select universal force field to optimize geometry using molecular dynamic method and minimized, finally the relationship between the macro-property and micro-structures is calculated using QSAR program. QSAR is a chemical structure-activity and structure-property statistical analytical method. The program can generate a large number (about 60) of molecular descriptors on the basis of the thermodynamic, geometrical and electronic structure of a molecule. The statistical analysis technique includes stepwise multiple linear regression analysis, generate multiple simple linear model analysis, multiple linear regression, and genetic function approximation analysis [16]. These analytical methods can be used to get a better relationship between the retention time and the micro-structures.

### 3. Results and discussion

#### 3.1. Chiral discrimination of organophosphonate derivatives by *N*-(3,5-dinitrobenzoyl)-leucine chiral stationary phase

Table 1 shows the retention factor and selectivity factor ( $\alpha$ ) of the organophosphonate derivatives enantiomers. All of the compounds can be baseline separated easily. A typical chromatograms for the chiral separation of compound 5 and 7 are shown in Fig. 3A and B, respectively. The  $k$  and  $\alpha$  values are decreased with increasing the concentration of isopropanol in mobile phase for all compounds. The order of chiral separation of substituent in para position of benzene ring was  $\alpha_{p-\text{OCH}_3} > \alpha_{p-\text{Cl}} > \alpha_{p-\text{CH}_3} > \alpha_{p-\text{NO}_2} > \alpha_{p-\text{H}}$ . When the same substituent is in different position

Table 1  
Retention factor ( $k$ ) and selectivity factor ( $\alpha$ ) of the organophosphonate derivatives enantiomers

Compound No.	R <sub>1</sub>	R <sub>2</sub>	2.5% isopropanol			5% isopropanol			10% isopropanol		
			$k_1$	$k_2$	$\alpha$	$k_1$	$k_2$	$\alpha$	$k_1$	$k_2$	$\alpha$
1	H	Et	4.222	6.130	1.452	2.186	3.037	1.389	1.103	1.450	1.315
2	<i>p</i> -OMe	Et	1.157	1.527	1.322 <sup>a</sup>	4.381	7.763	1.772	1.306	2.066	1.582
3	<i>p</i> -NO <sub>2</sub>	Et	1.651	2.322	1.407 <sup>a</sup>	5.174	7.995	1.545	2.263	3.217	1.421
4	<i>p</i> -Cl	Et	0.707	1.043	1.475 <sup>a</sup>	1.969	3.229	1.640	1.034	1.586	1.534
5	<i>o</i> -OMe	Et	9.496	12.408	1.307	4.576	5.812	1.270	2.198	2.666	1.213
6	<i>m</i> -Cl	Et	3.775	5.584	1.479	4.047	2.984	1.458	1.087	1.502	1.382
7	<i>m</i> -NO <sub>2</sub>	Et	2.054	2.966	1.444 <sup>a</sup>	6.050	9.606	1.588	3.096	4.616	1.491
8	<i>p</i> -Me	Et	4.086	6.357	1.556	2.269	3.511	1.548	1.413	1.657	1.451
9	<i>o</i> -Cl	Et	4.765	6.586	1.384	2.480	3.309	1.334	1.330	1.686	1.268
10	H	<i>i</i> -Pr	2.020	2.943	1.557	1.074	1.471	1.370	0.630	0.712	1.182
11	<i>p</i> -Cl	<i>i</i> -Pr	1.679	2.396	1.427	0.966	1.347	1.395	0.567	0.702	1.238
12	<i>p</i> -Cl	Me	1.294	1.826	1.411 <sup>a</sup>	4.002	6.065	1.515	1.976	2.831	1.433
13	H	Me	8.098	10.808	1.335	4.378	5.772	1.319	2.206	2.836	1.286
14	<i>p</i> -Cl	Pr	0.498	0.767	1.540 <sup>a</sup>	1.237	2.220	1.795	0.683	1.111	1.627
15	H	Pr	2.663	4.186	1.572	1.460	2.234	1.530	0.771	1.112	1.443

<sup>a</sup> The mobile phase was 15% isopropanol in *n*-hexane.

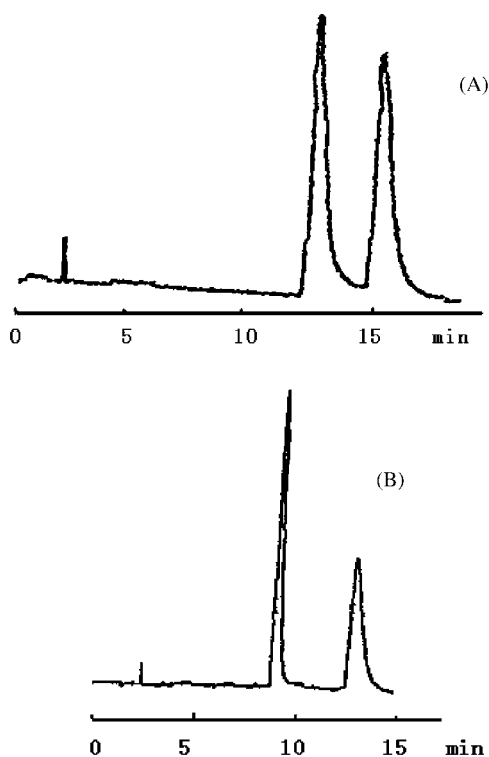


Fig. 3. Chromatograms of chiral separation of (A) compound 5; mobile phase: 5% of isopropanol in *n*-hexane and (B) compound 7; mobile phase: 10% of isopropanol in *n*-hexane.

of benzene ring, the orders are:  $\alpha_{p-Cl} > \alpha_{m-Cl} > \alpha_{o-Cl}$ ,  $\alpha_{p-OCH_3} > \alpha_{o-OCH_3}$ ,  $\alpha_{m-NO_2} > \alpha_{p-NO_2}$ . With different substituent  $R_2$ , and the substituent  $R_1$  is *p*-Cl, the  $\alpha$  values show an order of  $\alpha_{Pr} > \alpha_{Et} > \alpha_{Me} > \alpha_{i-Pr}$ . However, when the substituent  $R_1$  is H, the  $\alpha$  values show an order of  $\alpha_{Pr} > \alpha_{i-Pr} > \alpha_{Et} > \alpha_{Me}$ . We also performed the chiral separation of those organophosphonate derivatives by different polysaccharide-based chiral stationary phases with different mobile phase system [18–21]. The chiral discrimination

on these polysaccharide-based CSPs are based on  $\pi$ – $\pi$  interaction, H-bond interaction and the stereogenic fit in the chiral groove of these polysaccharide-based CSPs while the chiral discrimination in the case of *N*-(3,5-dinitrobenzoyl)-leucine (DNB-leu) CSP is based mainly on the  $\pi$ – $\pi$  interaction.

### 3.2. Study of chiral discrimination of organophosphonate derivatives by molecular modeling

With Cerius2 program, we can build the structures of CSP and the organophosphonate derivatives enantiomers. After building the structures, minimized energy is obtained under Universal 1.02 Force Field. The maximum number of interactions is 5000. For the interaction of organophosphonate derivatives and chiral stationary phase, we construct the two minimized structures separately at first, then, minimize the energy of the two molecules by auto-docking to get the energy of the complex. After 5000 steps at 0.0010 ps for each step of dynamics simulation at 300 K, we minimize the energy of the complex again to get the final energy of the complex of organophosphonate derivatives and chiral stationary phase.

Table 2 shows the energy of CSP, *R*- and *S*-enantiomers and the complex, respectively. From  $\Delta G_{CSP \cdot A-R}$  and  $\Delta G_{CSP \cdot A-S}$ , all the complexes of CSP·A-*R* have lower energy than CSP·A-*S* (Table 2). That means A-*R* form a more stable diastereomeric transient complex with the CSP. Accordingly, enantiomer of A-*R* should have longer retention time than enantiomer of A-*S*. Figs. 4 and 5 show the interaction between CSP and enantiomers of both *R* and *S* (CSP·A-*R* and CSP·A-*S*) of compound 1.

When using MM2, the energy of *R*-enantiomer was same as that of *S*-enantiomer [13]. In MM2, the force field treats the enantiomers totally as mirror symmetry molecules. The mirror is only at the chiral center, while the other part of the molecule does not possess symmetry. However, with

Table 2  
The energy of enantiomers and complex (kcal mol<sup>−1</sup>)

Compound No.	A- <i>R</i>	CSP·A- <i>R</i>	$\Delta G_{CSP \cdot A-R}$	A- <i>S</i>	CSP·A- <i>S</i>	$\Delta G_{CSP \cdot A-S}$
1	102.420	119.938	−22.0468	105.663	126.933	−18.2948
2	109.997	125.410	−24.1518	113.272	131.872	−20.9648
3	100.906	119.855	−20.6158	107.637	127.579	−19.6228
4	102.299	119.399	−22.4648	104.242	122.660	−21.1468
5	109.997	126.762	−22.7998	113.700	134.365	−18.8998
6	102.178	117.167	−24.5758	104.234	123.398	−20.4008
7	105.613	125.869	−19.3088	107.701	129.084	−18.1818
8	103.437	120.441	−22.5608	105.380	126.695	−18.2498
9	105.397	124.731	−20.2308	99.8830	123.874	−15.5738
10	99.7880	121.928	−17.4248	106.085	130.653	−14.9968
11	99.6307	122.642	−16.5535	105.951	129.178	−16.3378
12	98.7503	119.274	−19.0411	100.971	122.729	−17.8100
13	98.8606	120.265	−18.1604	103.467	129.686	−13.349
14	97.6166	116.126	−21.0554	105.043	124.297	−20.3108
15	103.371	120.466	−22.4698	104.644	127.396	−16.8128

The energy of CSP was 39.5648 kcal mol<sup>−1</sup>.

Table 3  
The final QSRR equations of organophosphonate derivatives<sup>a</sup>

	QSRR equations of stepwise predicted retention factors	$r^2$	$F$ -test
$R$ - $k_1$	$11.8234 + 0.078514 \times \text{"Vm"} - 0.146876 \times \text{"MW"} + 3.85429 \times \text{"H bond-acceptor"}$	0.904	34.518
$R$ - $k_2$	$14.7682 + 0.16822 \times \text{"Vm"} - 0.270454 \times \text{"MW"} + 6.60789 \times \text{"H bond-acceptor"}$	0.939	56.397
$S$ - $k_1$	$10.5144 + 0.201843 \times \text{"dipole-Z"} - 0.063819 \times \text{"MW"} + 3.69592 \times \text{"H bond-acceptor"}$	0.950	47.317
$S$ - $k_2$	$14.5709 + 0.16777 \times \text{"Vm"} - 0.27057 \times \text{"MW"} + 6.68347 \times \text{"H bond-acceptor"}$	0.938	55.017

<sup>a</sup> QSRR equations are based on  $k_1$  and  $k_2$  of the  $R$ - and  $S$ -enantiomers.

Cerius<sup>2</sup>, we found that the energy of  $R$ - and  $S$ -enantiomers is not same.

### 3.3. Study of retention behaviors of the enantiomers of organophosphonate derivatives by QSRR

We used QSRR to study the correlation between  $R$ - or  $S$ -enantiomers and the retention factor  $k_1$  and  $k_2$ . In QSRR, squared correlation coefficient (or coefficient of multiple determination),  $r^2$ , is a measure of the fit of the regression model. The correlation coefficient values closer to 1.0 represent a better fit of the model. The  $F$ -test reflects the ratio of the variance explained by the model and the variance due to the error in the model (i.e. the variance not explained by the model). High values of the  $F$ -test indicate that the model is statistically significant [22]. The stepwise multiple linear regression analysis in QSAR program is used to look for the best equation with the biggest squared correlation coefficient and  $F$ -test, which can be used to describe the relationship between the retention time and micro-structures.

The chromatographic system in this study was performed under normal phase mode. We study the correlation based on the parameters of energy (conformation), dipole (the dipole moment of molecule), HOMO (highest occupied molecular orbital energy), LUMO, MW (molecular weight), Vm (molecular volume) and Hf (thermodynamic). In the process of searching for the best equation, the equation with bigger  $r^2$  is selected when a single descriptor is considered. In this study, we used the structure parameters of  $S$ - and  $R$ -enantiomers to build the relationship equation with retention factor  $k_1$  and  $k_2$ . The bigger  $r^2$  is used to distinguish which equation fits to describe the retention factor. Finally, we got the equations with best correlation coefficient between retention time and microstructure which are shown in Table 3. The results indicate that  $R$ -enantiomers of organophosphonate derivatives have good correlation with  $k_2$  and  $S$ -enantiomers of organophosphonate derivatives have good correlation with  $k_1$ . This means  $R$ -enantiomers of organophosphonate derivatives have longer retention time than that of  $S$ -enantiomers. These results were same as the results obtained from molecular modeling.

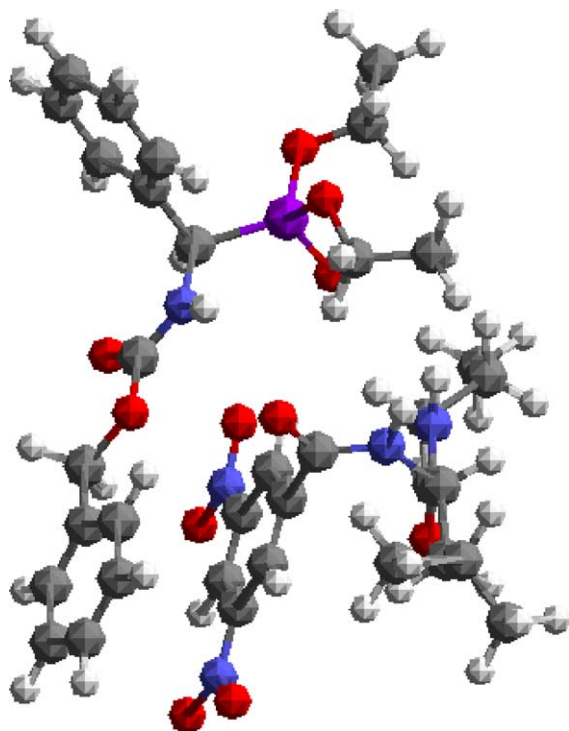


Fig. 4. The complex of CSP and  $R$ -enantiomer of compound 1 (CSP-A-R).

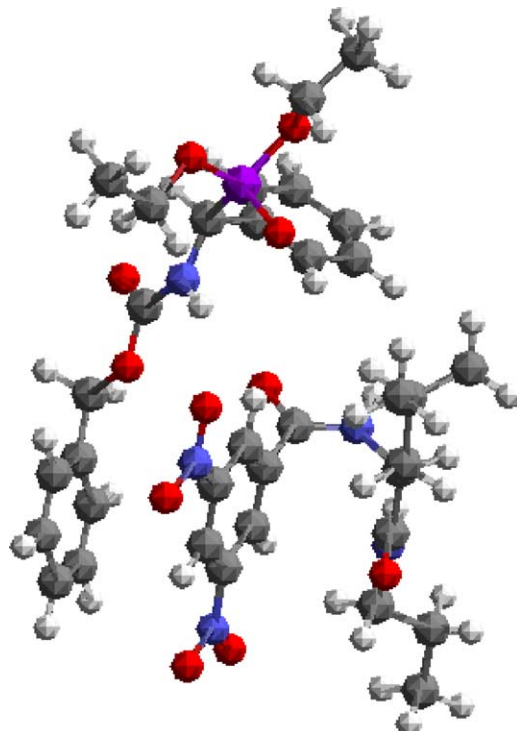


Fig. 5. The complex of CSP and  $S$ -enantiomer of compound 1 (CSP-A-S).



#### 4. Conclusions

Using molecular modeling, molecular dynamics, we can study the chiral discrimination leading to the resolution of organophosphonate derivatives enantiomers, by calculating the energy of the complex of CSP and enantiomers. Accordingly, one can predict the elution order of the enantiomers. Furthermore, the QSRR studies offers an alternative method to confirm the elution order of enantiomers. Molecular mechanics, molecular dynamics and QSRR can be useful methods to the study of chiral discrimination.

#### Acknowledgements

The project was supported by the National Natural Science Foundation of PR China (no. 20303011).

#### References

- [1] H.Y. Aboul-Enein, I. Ali, *Chiral Separation by Liquid Chromatography and Related Technologies*, Marcel Dekker, Inc., New York, USA, 2003.
- [2] H.Y. Aboul-Enein, I.W. Wainer, *The Impact of Stereochemistry on Drug Development and Use*, Wiley, New York, USA, 1997.
- [3] B. Chankvetadze, *Capillary Electrophoresis in Chiral Analysis*, Wiley, New York, USA, 1997.
- [4] J.H. Kennedy, *J. Chromatogr. A* 725 (1996) 219–224.
- [5] K.B. Lipkowitz, *J. Chromatogr. A* 906 (2001) 417–442.
- [6] K.B. Lipkowitz, *J. Chromatogr. A* 694 (1995) 15–37.
- [7] D.R. Taylor, K. Maher, *J. Chromatogr. Sci.* 30 (1992) 67–85.
- [8] M.G. Still, L.B. Rogers, *Talanta* 36 (1989) 35–48.
- [9] K.B. Lipkowitz, D.A. Demeter, R. Zegarra, R. Larter, T. Darden, *J. Am. Chem. Soc.* 110 (1988) 3446–3452.
- [10] K.B. Lipkowitz, B. Baker, R. Zegarra, *J. Comput. Chem.* 10 (1989) 718–732.
- [11] K.B. Lipkowitz, B. Baker, *Anal. Chem.* 62 (1990) 770–774.
- [12] K.B. Lipkowitz, S. Antell, B. Baker, *J. Org. Chem.* 54 (1989) 5449–5453.
- [13] G.S. Yang, B. Yan, L. Lei, W.-G. Wang, C.-B. Liu, *Chem. J. Chin. Universities* 21 (2000) 1745–1747.
- [14] Q. Dai, *Synthesis of a-(p-Toluenesulfonamideo)-Phosphonic Acid derivatives and Phosphonic Acid O-peptide and their Biological Activities*, National Laboratory of Elemento-Organic Chemistry, Nankai University, PR China, Ph.D. Thesis, 1995.
- [15] R.Y. Gao, G.S. Yang, H.X. Shen, R.Y. Chen, Q. Dai, Q.S. Wang, *J. Liq. Chromatogr. Rel. Technol.* 19 (1996) 171–178.
- [16] A.K. Rappe, C.J. Casewit, K.S. Colwell, W.A. Goddard III, W.M. Skiff, *J. Am. Chem. Soc.* 114 (1992) 10024–10035.
- [17] *QSAR User Guide*, San Diego, MSI, 1995.
- [18] W. Du, G.S. Yang, X.Q. Wang, S.L. Yuan, L. Zhou, D. Xu, C.B. Liu, *Talanta* 60 (2003) 1187–1195.
- [19] G.S. Yang, W. Du, L. Zhou, P. Piedad Vazquez, A. Garrido Frenich, J.L. Martine Vidal, H.Y. Aboul-Enein, *Anal. Lett.* 36 (7) (2003) 1423–1435.
- [20] G.S. Yang, P. Piedad Vazquez, A. Garrido Frenich, J.L. Martine Vidal, H.Y. Aboul-Enein, *Anal. Sci.* 19 (2003) 1157–1161.
- [21] G.S. Yang, P. Piedad Vazquez, A. Garrido Frenich, J.L. Martine Vidal, H.Y. Aboul-Enein, *J. Liq. Chrom. Rel. Technol.* 26 (2003) 3073–3082.
- [22] Y. Wang, X. Zhang, X. Yao, Y. Gao, M. Liu, Z. Hu, B. Fan, *Anal. Chim. Acta* 463 (2002) 89–97.